

High Resolution Prediction of Gas Injection Process Performance for Heterogeneous Reservoirs

Quarterly Report
April 1, 2003 to June 30, 2003

Contract No. DE-FC26-00BC15319

Principal Investigator: Franklin M. Orr, Jr.
Department of Petroleum Engineering
Stanford University

Disclaimer

This report was prepared as an account of work sponsored by an agency of the United States Government. Neither the United States Government nor any agency thereof, nor any of their employees, makes any warranty, express or implied, or assumes any legal liability or responsibility for the accuracy, completeness, or usefulness of any information, apparatus, product, or process disclosed, or represents that its use would not infringe privately owned rights. Reference herein to any specific commercial product, process, or service by trade name, trademark, manufacturer, or otherwise does not necessarily constitute or imply its endorsement, recommendation, or favoring by the United States Government or any agency thereof. The views and opinions of authors expressed herein do not necessarily state or reflect those of the United States Government or any agency thereof.

Abstract

This report presents a detailed analysis of the development of miscibility during gas cycling in condensates and the formation of condensate banks at the leading edge of the displacement front.

Dispersion-free, semi-analytical one-dimensional (1D) calculations are presented for enhanced condensate recovery by gas injection. The semi-analytical approach allows investigation of the possible formation of condensate banks (often at saturations that exceed the residual liquid saturation) and also allows fast screening of optimal injection gas compositions. We describe construction of the semi-analytical solutions, a process which differs in some ways from related displacements for oil systems.

We use an analysis of key equilibrium tie lines that are part of the displacement composition path to demonstrate that the mechanism controlling the development of miscibility in gas condensates may vary from first-contact miscible drives to pure vaporizing and combined vaporizing/condensing drives. Depending on the compositions of the condensate and the injected gas, multicontact miscibility can develop at the dew point pressure, or below the dew point pressure of the reservoir fluid mixture.

Finally, we discuss the possible impact on performance prediction of the formation of a mobile condensate bank at the displacement front in near-miscible gas cycling/injection schemes.

Table of Contents

1. Executive Summary	4
2. Introduction	5
3. Experimental	5
4. Mathematical Background	6
4. Solution construction for condensate displacements	7
4.1 Vaporizing drives.....	7
4.2 Development of miscibility in vaporizing drives	9
4.3 Combined condensing and vaporizing drives.....	9
5. Multicomponent Displacements.....	10
6. Results and Discussion.....	11
7. Conclusions	11
8. Nomenclature	12
9. References	12
10. Tables	14
11. Figures.....	16

1. Executive Summary

Gas cycling schemes for enhanced condensate recovery are inherently compositional because condensate is moved by transferring components to the mobile vapor phase. Hence, evaluation of the performance of such processes requires the use of compositional simulation. Recovery efficiency of a gas injection scheme is determined partly by the local displacement efficiency and partly by fluid flow within the reservoir. Local displacement efficiency is controlled by the phase behavior of mixtures of the injection gas with the fluids present in the reservoir, which is, in turn, strongly influenced by the fluid description used for equation-of-state calculations of phase behavior. Fluid flow is often controlled by reservoir heterogeneities. Therefore, accurate evaluation of the performance of a gas cycling scheme requires both high-resolution representation of heterogeneity in the reservoir and use of an adequate number of components to describe the phase behavior of the fluid.

FD compositional simulation is the conventional way to solve such problems. This approach involves solving a material balance written for each component, for each reservoir element (grid block), in each time step of the simulation, which requires at least one flash calculation per grid block per time step. For large models or complex fluid descriptions, this method can be sufficiently computationally expensive that field-scale calculations are impractically slow. In order to reduce computation time, current industry practice is to simplify the geological model and fluid description. As a result, there is clearly some loss of accuracy due to the less detailed representation of phase behavior and reservoir heterogeneities, as well as the effects of numerical errors due to large grid blocks.

We employ the analytical theory of gas injection processes to investigate the development of miscibility in gas cycling schemes. In other words we seek to understand the processes that lead to high local displacement efficiency in these displacement problems. Dispersion-free semi-analytical solutions to gas cycling schemes are presented and compared with fine and coarse grid finite difference simulations. The comparison clearly demonstrates the lack of accuracy of the coarse grid finite difference simulations. Consequently, the formation of a condensate bank at the leading edge of the displacement will only be described correctly when numerical artifacts are reduced to the what is physically realistic, a task that can only be achieved by our analytical approach or by running fine grid numerical simulations. The finite difference approach is unfeasible, however, due to the CPU requirement for these fine grid simulations.

Failing to describe the formation of condensate banks at the leading edge of the displacement may lead to incorrect conclusions as to the potential recovery from condensate fields. If the liquid saturation of the condensate bank exceeds the residual liquid saturation, gravity effects may very well cause the condensate to drop to the bottom of the formation and reduce the ultimate recovery from the reservoir.

2. Introduction

A significant portion of current hydrocarbon reserves exists in gas condensate carrying formations. In analog to oil reservoirs, production of condensate fields by primary production only will result in significant loss of the heavy ends due to liquid drop-out below the dew point pressure. Gas cycling/injection schemes are often applied to enhanced condensate recovery by vaporization. Successful design and implementation of enhanced condensate recovery schemes require accurate prediction of the compositional effects that control the local displacement efficiency.

Many contributions to the development of the analytical theory of gas injection processes can be found in the literature¹⁻¹¹. The previously published research in this field has been focused on the understanding and construction of analytical solutions to problems of gas displacing oil. In this work we extend the analytical theory to include the important process of enhanced condensate recovery by gas injection.

Numerical studies of miscibility variation in compositionally grading reservoirs by Hoier and Whitson¹² demonstrated a significant potential for efficient gas cycling in condensate reservoirs below the dew-point pressure due to the development of miscibility by the combined condensing and vaporizing mechanism. In their study, rich separator gas was injected to obtain a miscible displacement at pressures far below the dew-point pressure.

With the emerging focus and efforts in the area of greenhouse gas capture and sequestration, CO₂ may in the near future become widely available for enhanced oil recovery as well as enhanced condensate recovery projects. Seto *et al.*¹³ demonstrated, based on simulation studies, that CO₂ can be used as an effective solvent in enhanced condensate recovery processes at pressures well below the dew point pressure or the initial condensate.

In this report we focus on analyzing the development of miscibility during gas cycling in condensate reservoirs that after primary production leave significant amounts of retrograde condensate trapped in the formation.

We start out by presenting the conservation equations that describe multicomponent two-phase flow in a porous media including volume change on mixing and list the key assumptions made to apply the analytical solution strategy. We then describe, through analytical example calculations, the different mechanisms that control the development of miscibility in retrograde condensate reservoirs.

3. Experimental

This report describes the modeling work related to the development of miscibility in enhanced condensate recovery processes. Hence, no experimental work is reported.

4. Mathematical Background

The mass conservation equations for multicomponent, dispersion-free two-phase flow in one dimension can be written as

$$\frac{\partial G_i}{\partial \tau} + \frac{\partial H_i}{\partial \xi} = 0, \quad i = 1, \dots, n_c, \quad (1)$$

where G_i is the molar concentration of component i

$$G_i = x_i \rho_{xD} (1 - S) + y_i \rho_{yD} S, \quad (2)$$

and H_i is the molar flux of component i

$$H_i = u_D (x_i \rho_{xD} (1 - f) + y_i \rho_{yD} f). \quad (3)$$

Eqs. (1)-(3) are given in dimensionless form. The dimensionless form is obtained by introducing the variables

$$\tau = \frac{u_{inj} t}{\phi L}, \quad \xi = \frac{z}{L}, \quad \rho_{jD} = \frac{\rho_j}{\rho_{ini}}, \quad u_D = \frac{u}{u_{inj}}, \quad (4)$$

where u_{inj} is the injection velocity, t is the time, ϕ is the porosity and L is the overall length of the porous medium. The distance from the inlet is given by z and the molar density of the initial fluid is denoted ρ_{ini} . The phase equilibrium of the fluids are introduced in the flow equations by the molar density of phase j and the corresponding equilibrium vapor (y_i) and liquid (x_i) compositions of component i . Finally, S is the volumetric vapor phase saturation and f is the fractional flow of vapor related to S through

$$f = \frac{S^2}{S^2 + \mu_r (1 - S - S_{or})^2}. \quad (5)$$

In Eq. (5), μ_r is the ratio of vapor to liquid viscosity and S_{or} is the residual liquid saturation. Initial and injection states are specified by

$$Z_i(\xi, \tau = 0) = \begin{cases} Z_i^{inj}, & \xi < 0 \\ Z_i^{ini}, & \xi > 0 \end{cases}, \quad (6)$$

where Z_i is the overall mole fraction of component i and superscripts ini and inj signify initial and injection composition respectively. Eqs. 1-6 specify a Riemann problem and can be solved analytically provided that the gradient in pressure along the direction of the displacement is assumed to be negligible for the purpose of evaluating phase behavior.

Semi-analytical solutions to Eqs. 1 through 6 are constructed by the method of characteristics (MOC). The MOC rely on solving an eigenvalue problem associated with the mass conservation equations¹⁻¹¹. In composition space, the corresponding problem is to identify the correct (unique) route that connects the initial oil composition and the injection gas composition. A unique

composition path that describes the semi-analytical solution in composition space is subject to the following requirements.

Any composition path connecting injection and initial conditions must have characteristic wave velocities in the two-phase region that increase monotonically from upstream to downstream locations. This condition is also known as the velocity rule. A violation of the velocity rule by a continuous variation (rarefaction) allows multiple compositions to be found at the same location at the same time which is non-physical. In such cases a shock must be introduced to insure that the solution remains single-valued. The shock must satisfy the integral form of the mass conservation equations.

$$\Lambda = \frac{H_i^u - H_i^d}{G_i^u - G_i^d}, \quad i = 1, \dots, n_c, \quad (7)$$

where Λ is the shock velocity. Upstream and downstream sides of the shock are denoted u and d respectively. Eq. 7 is a Rankine-Hugoniot condition. Any shock present in a solution must be stable in the presence of a small amount of dispersion. This requirement is known as an entropy condition. In addition, solutions must satisfy a continuity condition with respect to initial and injection data. In other words, small perturbations to the initial or injection compositions must result in small changes in the solution.

4. Solution construction for condensate displacements

In the following sections we demonstrate the solution construction for enhanced condensate problems for three different fluid systems. All phase equilibrium calculations were performed using the Peng-Robinson equation of state while phase viscosities were calculated by the Lohrenze-Bray-Clark correlation.

4.1 Vaporizing drives

Consider the simple representation of a condensate given by a ternary mixture of methane (C_1), Ethane (C_2) and n-pentane (C_5) reported in Table 1. The phase envelope (PT-diagram) of the fluid is shown in Fig. 1. At a temperature of 325K this ternary system behaves like a retrograde condensate system below the dew-point pressure of 100 atm. To demonstrate how development of miscibility by a vaporizing mechanism develops, pure C_1 is injected into the condensate at 75 atm ($S_{or} = 0$). The binodal curve corresponding to a pressure of 75 atm along with the location of the initial and injected composition is shown on a ternary diagram in Fig. 2. From the analytical theory of gas injection processes¹⁻⁶, we know that the composition path connecting the initial and injection compositions must pass through a sequence of $n_c - 1$ key tie lines. For ternary displacements the key tie lines are the initial tie line and the injection tie line. The initial tie line extends through initial fluid composition, or in the case of a two-phase initial condition: the initial tie line is given directly by a PT-flash calculation. And, the injection tie line is the tie line that extends through the injection composition. Both key tie lines are shown in Fig. 2. A sketch of the fractional flow curves corresponding to the initial and injection tie lines is shown in Fig. 3. The solution path connecting the initial tie line to the injection tie line must in this case be a shock. This particular solution structure is a direct result of the orientation of the key tie lines and the envelope rule¹¹. The envelope rule states that for vaporizing displacement with a vapor-side

envelope curve (the curve which is tangent to the extensions of all tie lines in the surface spanned by the key tie lines) the key tie lines must be connected by a shock for the solution to stay single-valued. Johns *et al.*² and Birol *et al.*³ proved that two tie lines that are connected by a shock must intersect. This observation allow us to write the shock balance as

$$\Lambda = \frac{H_i^a - H_i^b}{G_i^a - G_i^b} = \frac{H_i^a - H_i^x}{G_i^a - G_i^x} = \frac{H_i^b - H_i^x}{G_i^b - G_i^x}, \quad i = 1, \dots, nc, \quad (8)$$

where superscript a , b denote the different sides of the shock and x denotes the intersection point. The graphical interpretation of Eq. (8) is shown in Fig. 3. The limiting case demonstrated in Fig. 3 corresponds to the highest saturation of the initial fluid for which it is possible to determine the shock velocity be a Welge tangent construction. For all condensate displacements studied throughout this report, the initial composition is located between the limiting composition and the equilibrium vapor composition, and hence the shock velocity is determined by a direct jump from the initial composition to the neighboring tie line. The only question remaining before solving this ternary displacement problem is how to deal with the change in the total flow velocity across the shock. In the formulation of the conservation equations we scaled the total flow velocity with respect to the injection velocity. Hence, the injection composition corresponds to a dimensionless velocity of one. As we start the solution construction at the downstream end of the displacement, we do not know the total velocity that enters the shock balance equations (Eq. 8). To overcome this problem, we rescale the conservation equations with respect to the velocity of the compositions on the initial tie line (the total velocity is constant for composition changes along a given tie line within the two-phase region). To calculate the shock velocity we locate the intersection point and evaluate the overall molar concentration by

$$\Lambda_{a,b} = \frac{H_1^a - H_1^x}{G_1^a - G_1^x} = \frac{H_1^a - G_1^x}{G_1^a - G_1^x} \quad (9)$$

with

$$G_1^x = x_1^a \rho_x^a (1 - \theta) + y_1^a \rho_y^a \theta \quad (10)$$

where θ is the fictive saturation corresponding to the intersection point measured from the initial tie line. The landing point and the total velocity on the injection tie line are then evaluated by the shock balances for C_1 and C_5 . The injection composition is connected to the landing point on the injection tie line by a direct jump as a tangent construction would violate the velocity rule as seen from Fig. 3. Hence, the total velocity corresponding to the injection composition (rescaled value) can be found from the shock balance equation. A final transformation to rescale all shock velocities with respect to the injection velocity is required to obtain the full solution. The analytical solution is shown on the ternary diagram (Fig. 2) and is reported in terms of saturation and composition profiles along with a finite difference (FD) simulation using 100 grid blocks in Fig. 4. Tabulated values are given in Table.2.

4.2 Development of miscibility in vaporizing drives

The solution to the displacement of the ternary condensate by pure Methane at 75 atm and 325K is clearly not a miscible displacement (piston like). If we slide the initial composition along the initial tie line, the slope of the line that connects the intersection point to the initial compositions increases. The slope of this line is equivalent to the shock speed of the leading edge of the displacement. Hence, to achieve a piston like displacement we must move the initial composition all the way to the vapor locus of the binodal curve at which point, the shock speed will be equal to one. Alternatively, we can increase the pressure to obtain the same effect. Fig. 2 shows a second binodal curve corresponding to a pressure of 100 atm. As we increase the pressure from 75 atm to 100 atm the binodal curve moves closer to the initial composition. As the binodal curve reaches the initial composition a piston-like displacement is achieved, and the displacement is multicontact miscible. If we increase the pressure above the dew point pressure the displacement switches from multicontact miscible to first contact miscible. This is not necessarily the case for all vaporizing drives. If the dilution line, connecting the initial composition to the injection composition, intersects the two-phase region at pressures above the dew point pressure, the displacement will still be multicontact miscible, but at a pressure above the minimum miscibility pressure (MMP), because the initial composition lies outside the region of tie-line extensions.

The development of miscibility described for the ternary displacement is valid also for multicomponent vaporizing drives. This due to the fact that the initial tie line controls the development of miscibility in any given vaporizing displacement.

4.3 Combined condensing and vaporizing drives

To illustrate the development of multicontact miscibility in combined condensing/vaporizing (C/V) displacements of condensate we turn to the 4-component system described in Table 3. The condensate is made up by 80% (mole) CH₄, 15% n-butane (C₄) and 5% decane (C₁₀) and we inject pure CO₂ (S_{or} = 0.2). The phase envelope of the condensate is given in Fig. 5. At a temperature of 344K the fluid system represents a near-critical condensate. A significant difference between ternary and quaternary displacement is the introduction of a third key-tie line know as a crossover tie line¹. Johns *et al.*² demonstrated that the crossover tie line is responsible for the development of combined C/V miscibility as reported by Zick¹⁴ and Stalkup¹⁵.

It is well known that miscibility for gas/oil displacements can develop by the C/V mechanism at pressures far below the vaporizing drive. Hoier and Whitson¹² demonstrated the similar behavior for the displacement of retrograde condensate by injection of a rich gas. In the following example calculation we demonstrate the similar behavior for CO₂ injection. To generate a semi-analytical solution to the displacement of the condensate by pure CO₂ we set the pressure to 100 atm (P_{dew} = 228 atm). The key tie lines that make up the solution in composition space can be located¹⁶⁻¹⁸ by applying the tie-line intersection equations.

Once the key tie lines are located (See Fig. 6) the solution strategy from the ternary displacement example is repeated. We start by connecting the initial composition to the crossover tie line by evaluating the shock velocity from the information about the tie-line intersection point. As in the previous example calculation we, rescale the shock velocities with respect to the total velocity of the compositions on the initial tie line. Knowing the landing point on the crossover tie line we construct the shock from the crossover to the injection tie line also like in the ternary displacement. In essence, solving a quaternary displacement problem

corresponds to solving two coupled ternary displacement problems. The solution path for the quaternary displacement is shown in Fig. 6 whereas the saturation and composition profiles are shown in Fig. 7 together with coarse and fine grid FD simulations. Tabulated results are given in Table 4.

A major difference in the solution profiles is seen for the quaternary C/V displacement relative to the pure vaporizing ternary displacement. At the leading edge of the displacement, a condensate bank is formed with high concentration of C_4 and CO_2 . In this case the retrograde liquid saturation of the bank exceeds the residual liquid saturation and hence becomes mobilized. The condensate bank is a result of the location of the landing point on the crossover tie line that is closer to the critical locus than is the initial or the injection tie line. If we increase the pressure the condensate bank shrinks in width and grows in height until the point where the crossover tie line becomes critical (zero length tie line) and a piston-like displacement develops. The pressure at which the crossover tie line becomes critical is the C/V MMP. From Fig. 6 it is clear that C/V miscibility will be much lower than the dew point pressure (228 atm) of the condensate.

Another interesting feature of the C/V drive can be deduced from Fig. 6. Hoier and Whitson¹² found, from numerical simulations, that the MMP of a C/V drive could be determined from the composition of the retrograde liquid and the injection gas composition. Their finding is consistent with the analytical theory as the retrograde liquid will specify the initial tie line.

5. Multicomponent Displacements

To test the new approach for generating semi-analytical solutions to condensate displacement problems on a multicomponent reservoir fluid, we select the fluid reported by Seto *et al.*¹³. Based on the equation of state input is given in Table 5, the phase envelope shown in Fig. 8 was generated. The reservoir fluid is represented by 13 components and again we use pure CO_2 as injection gas. First we consider the displacement of condensate at 335 K to achieve a near-critical reservoir fluid. The dew point pressure of the initial fluid is 158 atm and the MMP predicted by the key tie line approach is 93 atm.

To generate the solution we locate the key tie lines¹⁶⁻¹⁸ at 90 atm. In a 13 component system, there exist n_c-1 key tie lines, out of which n_c-3 are crossover tie lines. Hence, the construction of the analytical solution corresponds to solving 10 coupled pseudo-ternary displacements, starting from the initial tie line through to the injection tie line. For the fluid system in consideration the second crossover tie line controls the development of miscibility and hence, the displacement is a C/V drive. The full solution to the displacement of the retrograde condensate at 90 atm ($S_{or} = 0.2$) is tabulated in Table 6 and shown in terms of saturation and composition profiles in Fig. 9. Additional FD simulations are reported in Fig. 9 also. At the leading edge of the displacement we see a significant condensate bank that by far exceeds the residual saturation of 0.2. However, by inspecting the phase envelope we should expect significant changes in saturation as small variations in the initial composition will bring relatively large variations in saturation.

To investigate the significance of the initial composition relative to the critical point (temperature) we repeat the displacement problem at 375K (moving right in the phase envelope). At this temperature the dew-point pressure is 167 atm and the MMP is predicted to 128 atm. The dispersion-free solution for this displacement problem is reported in Fig. 10. The solution shows a significantly smaller condensate bank that hardly exceeds the residual saturation. Hence, the location of the initial condensate relative to the critical point on the phase envelope and hence the

0.5 quality line appears to have a significant impact on the formation of a condensate bank at the leading edge of the displacement.

6. Results and Discussion

In the previous sections we have applied the analytical theory of gas injection processes to predict the displacement behavior of gas injection into retrograde condensates. One of the major assumptions of this approach is to neglect the gradient in pressure for the purpose of evaluating phase behavior. Hence, semi-analytical predictions should not be expected to be highly accurate in near-well settings where steep gradients in pressure certainly exist. However, far from production wells, important information about the expected behavior of an enhanced condensate recovery scheme may still be at hand. The formation of condensate banks that exceed the residual liquid saturation suggests that gravity segregation could reduce displacement performance by draining valuable retrograde liquid away from high permeable zones at the cost of a reduction in recovery. To accurately predict the extent of a condensate bank we have demonstrated that significant grid refinement is required. Hence, coarse grid simulation of field development scenarios may fail to predict the true effects of gravity in these flow settings.

7. Conclusions

The examples and analysis presented in this report establish that:

1. The analytical theory of gas displacement can be used to describe enhanced condensate recovery by gas injection. Semi-analytical dispersion-free 1D solutions to 3-, 4- and 13-component fluid descriptions have been presented. The presented analytical solutions are in excellent agreement with fine grid numerical simulations. However, coarse grid numerical simulations fail to capture the formation of condensate banks.
2. Development of miscibility in gas cycling schemes may be achieved at pressures far below the dew-point pressure of the condensate by injection of CO₂.
3. Formation of a condensate bank at the leading edge of the displacement for C/V drives is reported. The magnitude of the saturation change in the condensate bank is related to the location of the initial condensate with respect to the critical point of the original condensate.
4. The fairly low miscibility pressures obtained for injection of CO₂ in a retrograde condensate suggests that mature condensate carrying formations may be suitable targets for CO₂ sequestration offset by a possible increase in condensate recovery.

8. Nomenclature

f	<i>Fractional flow of vapor</i>
G_i	<i>Molar concentration of component i</i>
H_i	<i>Molar flux of component i</i>
L	<i>Total length of system</i>
n_c	<i>Number of components</i>
S	<i>Gas saturation</i>
S_{or}	<i>Residual liquid saturation</i>
t	<i>Time</i>
u	<i>Total velocity</i>
u_D	<i>Dimensionless total velocity</i>
u_{inj}	<i>Injection velocity</i>
x_i	<i>Mole fraction of component i in liquid phase</i>
y_i	<i>Mole fraction of component i in vapor phase</i>
z	<i>Distance from inlet</i>
Z_i	<i>Overall mole fraction of component i</i>
ϕ	<i>Porosity</i>
Λ	<i>Shock speed</i>
μ_r	<i>Gas to oil viscosity ratio</i>
θ	<i>Fictive saturation at intersection point</i>
ρ_x	<i>Molar density of liquid</i>
ρ_y	<i>Molar density of vapor</i>
ρ_j	<i>Molar density of phase j</i>
ρ_{jD}	<i>Dimensionless density of phase j</i>
ρ_{ini}	<i>Molar density of initial fluid</i>
τ	<i>Dimensionless time (PVI)</i>
ξ	<i>Dimensionless length</i>

9. References

1. Monroe, W.W. et al.: "Composition Paths in Four-Component Systems: Effect of Dissolved Methane on 1D CO₂ Flood Performance," SPERE (August 1990) 423.
2. Johns, R.T., Dindoruk, B., and Orr, F.M., Jr.: "Analytical Theory of Combined Condensing/Vaporizing Gas Drives," SPE Advanced Technology Series (1993) 2, 7.
3. Dindoruk, B. Johns, R.T. and Orr, F.M., Jr. "Analytical solutions for Four Component Gas Displacements with Volume Change on Mixing" ECMOR III, Delft, Holland, 1992
4. Johansen, T., Dindoruk, B., and Orr, F.M., Jr.: "Global Triangular Structure in Four-Component Conservation Laws," Proc., Fourth European Conference on the Mathematics of Oil Recovery, Roros, Norway (1994).
5. Johns, R.T. and Orr, F.M., Jr.: "Miscible Gas Displacement of Multicomponent Oils," SPEJ (March 1996) 39.
6. Dindoruk, B., Orr, F.M., Jr., and Johns, R.T.: "Theory of Multicontact Miscible Displacement with Nitrogen," SPEJ (September 1997) 268.

7. Dindoruk, B.: "Analytical Theory of Multiphase, Multi-component Flow in Porous Media," Ph.D. dissertation, Stanford U., Palo Alto, California (1992).
8. Helfferich, F.G.: "Theory of Multicomponent, Multiphase Displacement in Porous Media," *SPEJ* (February 1981) 51.
9. Zanotti, F., De Notaristefani, C., and Gardini, L., "Sharpening Behavior of Chemical Flooding," SPE 11809 available from SPE, Richardson, Texas (1983).
10. Cere', A. and Zanotti, F. "Sharpening Behaviour and Dispersion in Chemical Flooding," *Proc.*, Third European Meeting on Improved Oil Recovery, Rome (1985).
11. Jessen, K., Wang, Y., Ermakov, P., Zhu, J., and Orr, F.M., Jr.: "Fast, Analytical Solutions for 1D Multicomponent Gas Injection Problems," SPE 74700, SPEJ, Dec 2001.
12. Hoier, L. and Whitson, C. H.: "Miscibility Variation in Compositionally Grading Reservoirs", SPE REE, February 2001.
13. Seto, C.J, Jessen, K. and Orr, F.M. Jr.: "Compositional Streamline Simulation of Field Scale Condensate Vaporization by Gas Injection", SPE 79690, SPE Reservoir Simulation Symposium, Houston, TX, February 3-5, 2003.
14. Zick, A.A.: "A Combined Condensing?Vaporizing Mechanism in the Displacement of Oil by Enriched Gases", SPE15493, ATCE, New Orleans, LA, 1986.
15. Stalkup, F.I. "Displacement Behavior of the Condensing/Vaporizing Gas Drive Process", SPE 16715, ATCE, Dallas, TX, 1987.
16. Jessen, K., Michelsen, M.L., and Stenby, E.H.: "Global Approach for Calculation of Minimum Miscibility Pressure," *Fluid Phase Equilibria* (1998) **153**, 251.
17. Wang, Y. and Orr, F.M., Jr.: "Calculation of Minimum Miscibility Pressure," *J. Pet. Sci. Eng.* (2000) **27**, 151.
18. Yuan, H. and Johns, R.T.: "Simplified Method for Calculation of Minimum Miscibility Pressure or Enrichment", SPE 77381, ATCE, San Antonio, Texas, 29 September-2 October 2002.

10. Tables

Component	T_c (K)	P_c (atm)	Ω	M_w (g/mole)	Z_c	$z_{\text{condensate}}$
Methane	190.6	45.389	0.0080	16.043	0.2896	0.5
Ethane	305.4	48.083	0.0980	30.070	0.2818	0.4
n-Pentane	465.9	33.340	0.2413	72.150	0.2685	0.1

Table 1: EOS parameter for the ternary displacement. All $K_{ij} = 0$

Segment	$\lambda (= z/t)$	S_{gas}	v_d	z_{C1}	z_{C2}	z_{C5}
1	0.9551 - ∞	0.9515	1.0488	0.5	0.4	0.100
2	0.9551 - 0.6222	0.9762	1.0246	0.888	0.0	0.112
3	0.6222 - 0	1.0000	1.0000	1.000	0.0	0.000

Table 2: MOC solution for ternary displacement

Component	T_c (K)	P_c (atm)	Ω	M_w (g/mole)	Z_c	$z_{\text{condensate}}$
C_1	190.6	45.389	0.0115	16.043	0.2896	0.80
CO_2	304.2	72.865	0.2236	44.010	0.2709	0.00
n- C_4	425.1	37.464	0.2002	58.123	0.2730	0.15
n- C_{10}	617.7	20.824	0.4923	142.29	0.2474	0.05

Table 3: EOS parameter for the quaternary displacement. Non-zero K_{ij} : $K_{CO_2,C_4} = 0.12$, $K_{CO_2,C_{10}} = 0.115$

Seg.	$\lambda (= z/t)$	S_{gas}	v_d	z_{C1}	z_{CO_2}	z_{C_4}	$z_{C_{10}}$
1	0.9325 - ∞	0.8994	0.9133	0.8000	0.0000	0.1500	0.05
2	0.9325 - 0.7076	0.7215	0.9691	0.0000	0.8301	0.1307	0.0393
3	0.7076 - 0.1918	0.929	0.9693	0	0.9586	0	0.0414
4	0.1918 - 0	1	1	0	1	0	0

Table 4: MOC solution for quaternary displacement

Comp.	z_{cond}	T_c (K)	P_c (atm)	Ω	M_w (g/mole)	Z_c
N2	0.0171	126.2	33.60	0.0400	28.016	0.287050
CO2	0.0576	304.2	72.90	0.2280	44.010	0.270553
H2S	0.3562	373.5	88.50	0.0800	34.076	0.283540
Methane	0.3631	190.6	45.40	0.0080	16.043	0.289858
Ethane	0.0798	305.4	48.20	0.0980	30.069	0.281961
Propane	0.0340	369.8	41.90	0.1520	44.096	0.277222
Butane	0.0300	419.6	37.01	0.1875	58.123	0.274107
Pentane	0.0171	465.9	33.34	0.2413	72.150	0.269386
C6	0.0116	507.4	29.30	0.2960	86.177	0.264586
C7	0.0117	573.9	40.47	0.2651	94.000	0.267297
C8	0.0126	648.3	32.53	0.3437	113.52	0.260400
C10	0.0053	630.1	30.17	0.4489	141.52	0.251169
C12+	0.0039	683.2	26.92	0.6305	190.00	0.235234

Non-zero K_{ij} : $N_2-C_1 = 0.02$, $N_2-C_2 = 0.06$, $N_2-C_{3+} = 0.08$, $CO_2-H_2S = 0.12$, $CO_2-C_1 = 0.12$, $CO_2-C_{2+} = 0.15$, $H_2S-C_1 = 0.08$, $H_2S-C_2 = 0.07$, $H_2S-C_3 = 0.07$, $H_2S-C_4 = 0.06$, $H_2S-C_5 = 0.06$, $H_2S-C_6 = 0.05$,

Table 5: EOS parameter for the 13 component displacement.

Seg.	$\lambda (= z/t)$	S_{gas}	v_d	z_{CO_2}
1	0-0.0855	1	1	1
2	0.0855-0.1616	0.9927	0.9965	0.9929
3	0.1616-0.1665	0.9777	0.9872	0.9761
4	0.1665-0.3799	0.9763	0.9863	0.9740
5	0.3799-0.5602	0.9687	0.9795	0.9604
6	0.5602-0.6644	0.957	0.9712	0.9431
7	0.6644-0.7570	0.9452	0.9663	0.9207
8	0.7570-0.8270	0.9232	0.9644	0.876
9	0.8270-0.8350	0.8737	0.9719	0.7884
10	0.8350-0.9256	0.7378	1.065	0.594
11	0.9256-0.9809	0.5817	1.0771	0.4886
12	0.9809-1.024	0.8949	0.9748	0.0582
13	1.024- ∞	0.8966	0.9723	0.0576

Table 6: MOC solution for near-miscible 13 component displacement

11. Figures

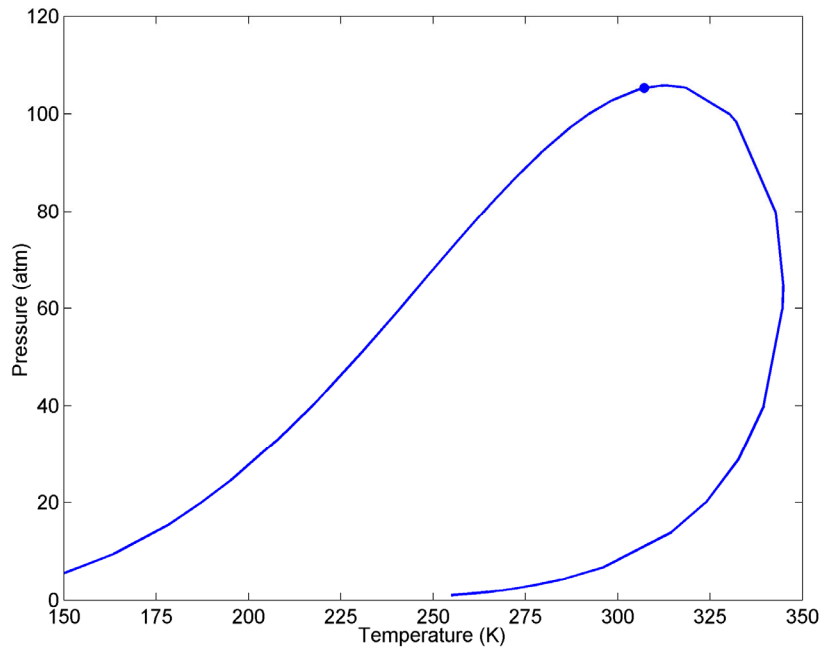


Figure 1: Phase envelope of ternary C₁/C₂/C₅ mixture. Near-critical retrograde behavior at 325 K

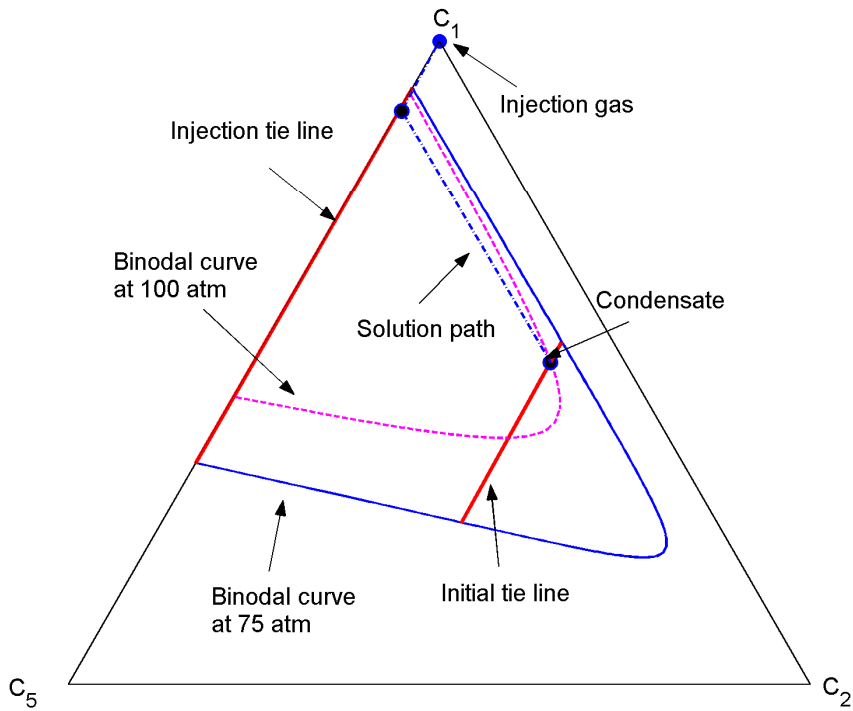


Figure 2: Displacement of 3 component condensate by pure C₁ at 325 K and 75 atm (MMP = P_{dew} = 100 atm)

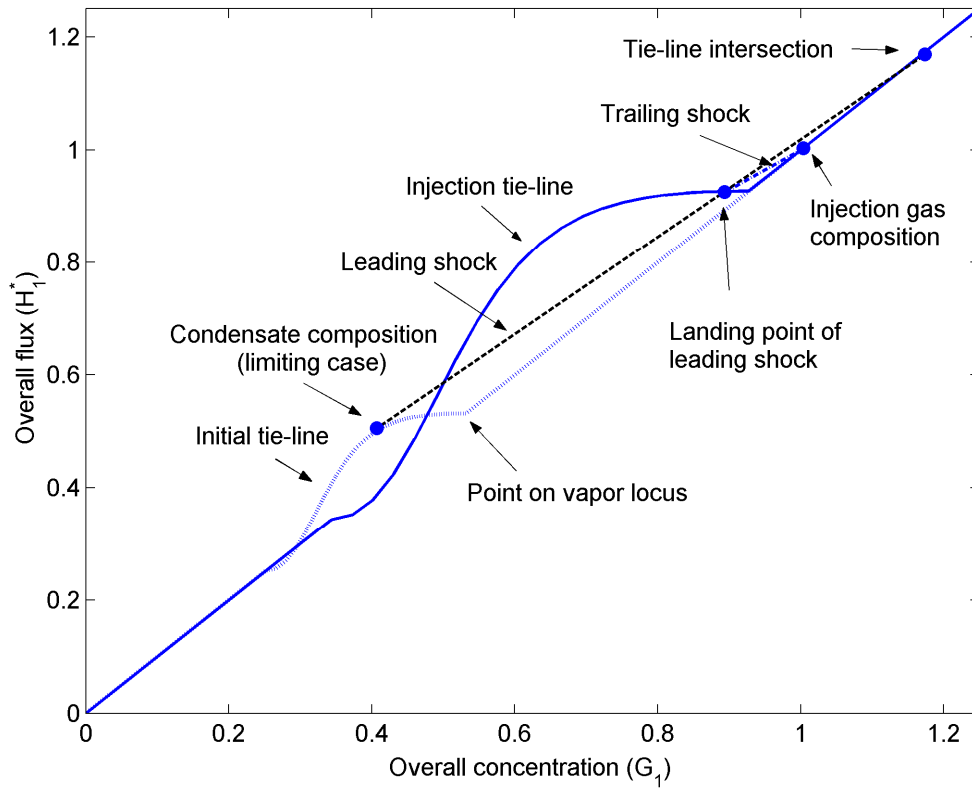


Figure 3: Displacement of 3 component condensate by pure C_1 at 325 K and 75 atm ($MMP = P_{dew} = 100$ atm)

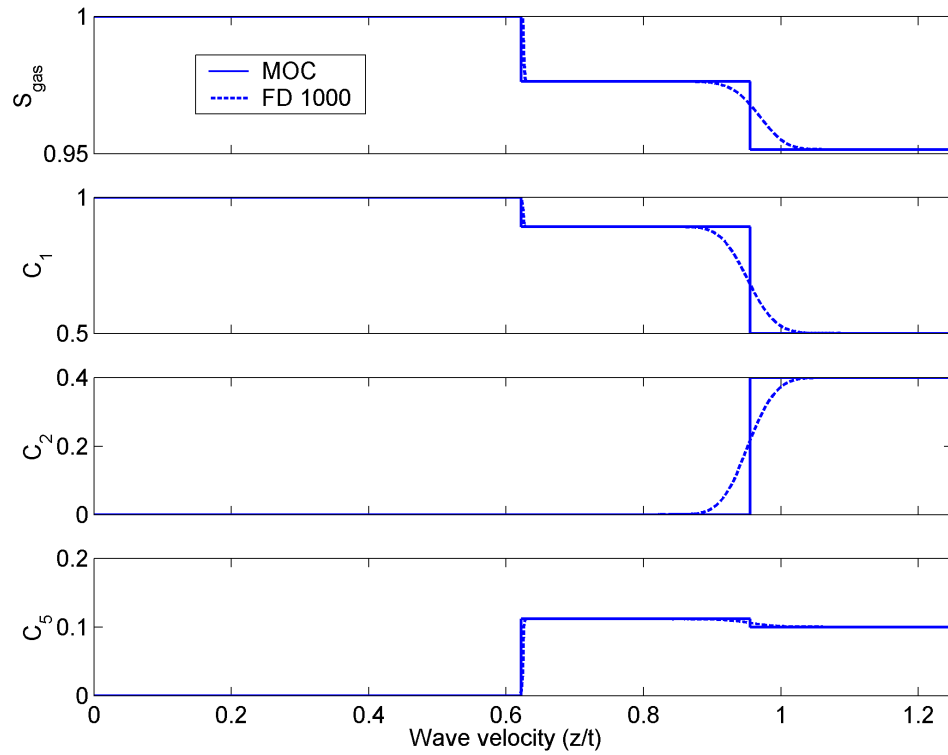


Figure 4: Semi-analytical and numerical (1000 grid blocks) solution profiles for the displacement of a 3 component condensate by pure C_1 at 75 atm and 325 K

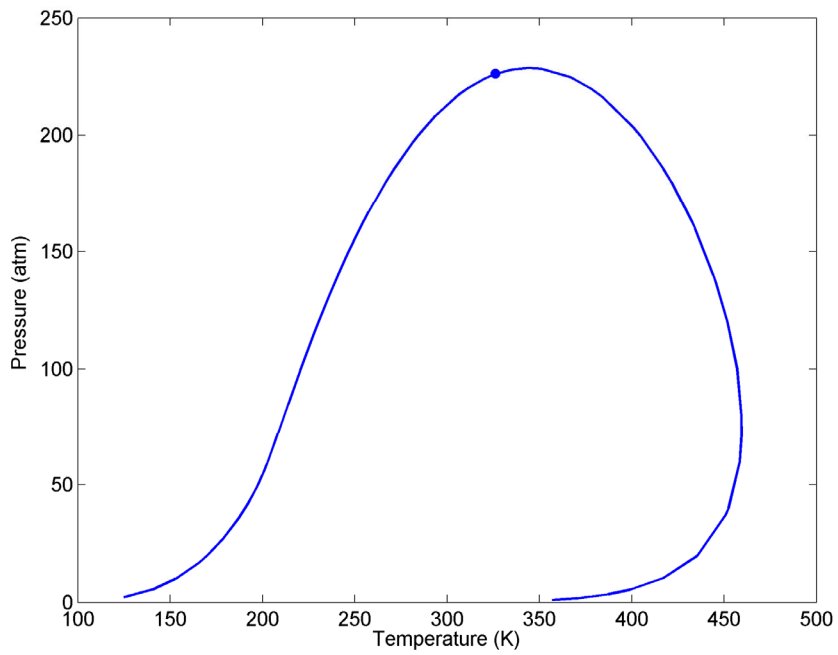


Figure 5: Phase envelope of 4 component mixture. Near-critical retrograde behavior at 344 K

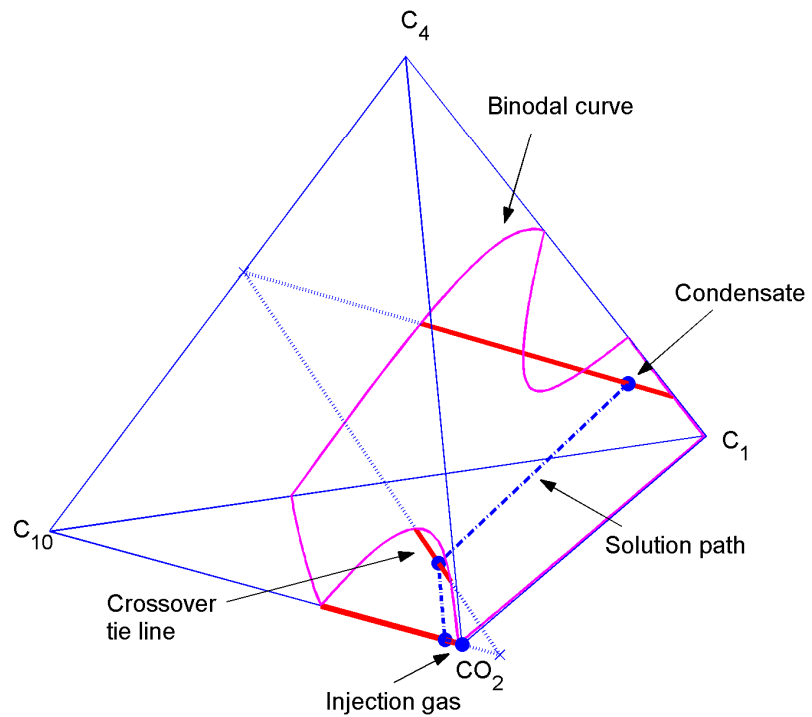


Figure 6: Near-miscible displacement of 3 component condensate by pure CO₂ (4 components) at 344 K and 100 atm (MMP = 106 atm)

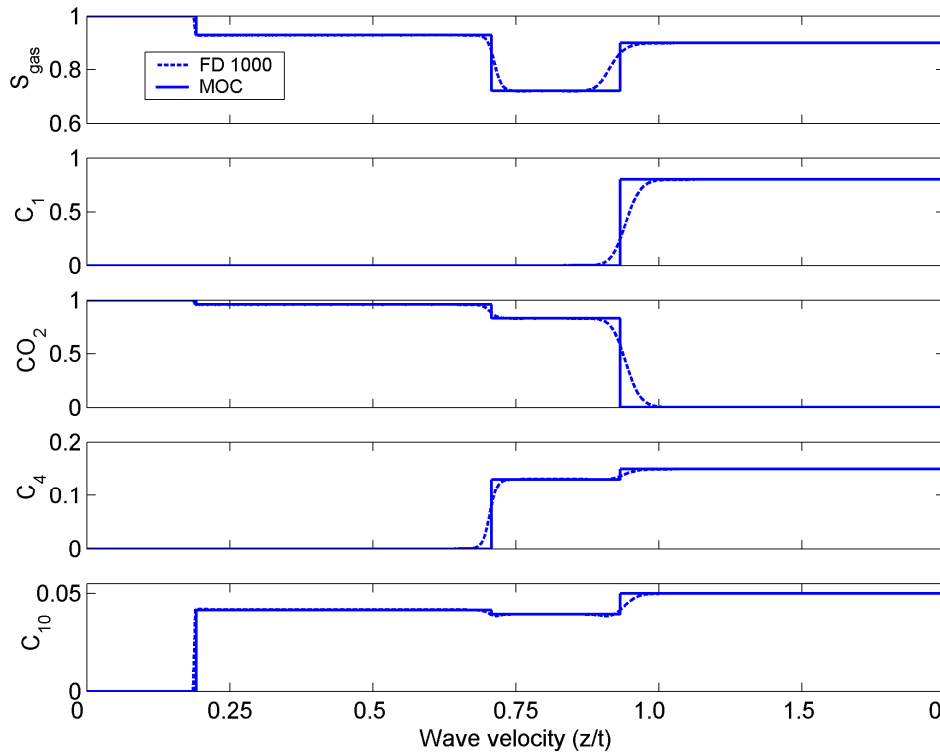


Figure 7: Semi-analytical and numerical (1000 grid blocks) solution profiles for the displacement of a 4 component condensate by pure CO_2 at 100 atm and 344 K

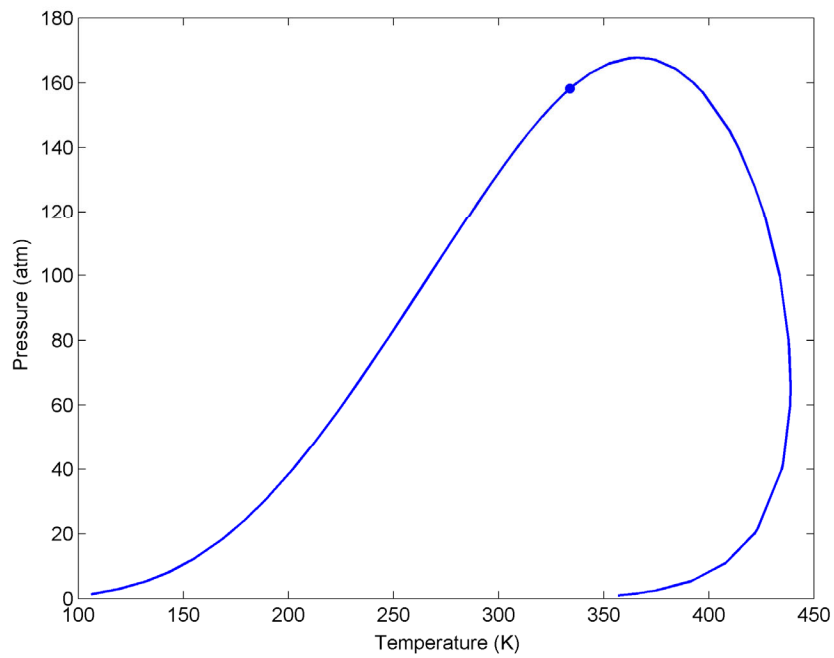


Figure 8: Phase envelope of 13 component mixture. Near-critical retrograde behavior at 335 K

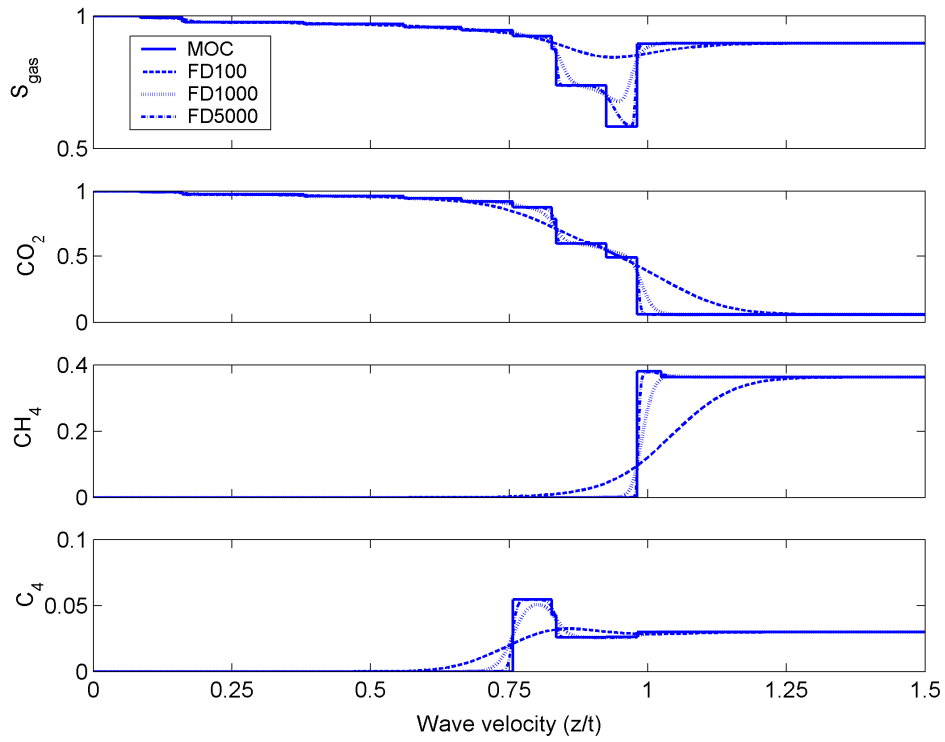


Figure 9: Semi-analytical and numerical solution profiles for the displacement of a 13 component condensate by pure CO₂ at 90 atm and 335 K (MMP = 93atm)

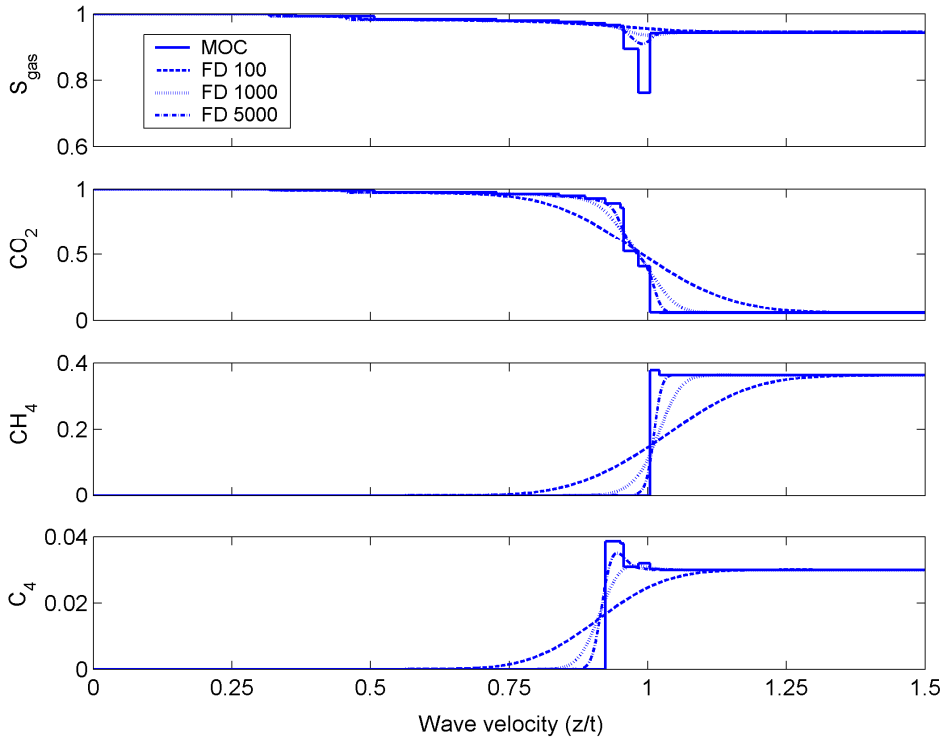


Figure 10: Semi-analytical and numerical solution profiles for the displacement of a 13 component condensate by pure CO₂ at 126 atm and 375 K (MMP = 128 atm)